

High-Speed Measurement of BRDF using an Ellipsoidal Mirror and a Projector

Yasuhiro MUKAIGAWA Kohei SUMINO Yasushi YAGI
The Institute of Scientific and Industrial Research, Osaka University
8-1 Mihogaoka, Ibaraki, Osaka, 567-0047, Japan
mukaigaw@am.sanken.osaka-u.ac.jp

Abstract

Measuring BRDF (Bi-directional Reflectance Distribution Function) requires huge amounts of time because a target object must be illuminated from all incident angles and the reflected lights must be measured from all reflected angles. In this paper, we present a high-speed method to measure BRDFs using an ellipsoidal mirror and a projector. Our method makes it possible to change incident angles without a mechanical drive. Moreover, the omni-directional reflected lights from the object can be measured by one static camera at once. Our prototype requires only fifty minutes to measure anisotropic BRDFs, even if the lighting interval is one degree.

1. Introduction

Measuring the 3-D shape of real objects is not a difficult problem if a range finder is used. On the other hand, measuring the reflection properties of real objects, however, remains a difficult problem. Reflection properties depend on the microscopic shape of the object surface, and they can be used for many applications such as computer graphics, archiving cultural heritages, and object recognition. However, there is no simple type of equipment that can measure reflection properties.

The main reason for this is that the dense measurement of BRDFs (Bi-directional Reflectance Distribution Functions) requires huge amounts of time because a target object must be illuminated from every incident angle and the reflected lights must be measured from every reflected angles. Hence, most existing methods simplify the problem by approximating the BRDF as a parametric function or assuming a uniform BRDF over the surface. As a result, complex reflection properties cannot be accurately measured.

In this paper, we straightforwardly tackle the problem of measuring dense BRDFs without any simplifications. Our system substitutes an ellipsoidal mirror for a mechanical

drive, and a projector for a light source. Since our system completely excludes mechanical rotation and translation, high-speed measurement can be realized.

2. Related works

For descriptions of reflection properties, several parametric models, such as the Phong model[9] and Torrance-Sparrow model[11], have been widely used. To approximate the reflection properties of real objects using these parametric models, parameter estimation is necessary. Sato et al.[10] proposed a method for estimating parameters of the Torrance-Sparrow model based on the 3-D shape and real images of the object. Machida et al.[7] proposed a method for densely estimating parameters of the Torrance-Sparrow model while taking interreflections into account. However, these parametric models have a common drawback in that complex reflection properties cannot be accurately expressed.

Recently, non-parametric models are becoming mainstream with the increasing storage capacities of PCs. Non-parametric models do not approximate reflection properties with mathematical formulations but directly record appearance for every lighting direction. Furthermore, if the lighting direction is sufficiently dense, even complex reflectance properties can be recorded without any errors. Debevec et al.[3] constructed the ‘Light Stage’ system, which can measure face appearances with changing light directions. The system has also improved in speed by incorporating a high-speed camera and flashes[5]. Moreover, they constructed a LED-based lighting environment that can reproduce arbitrary illuminations [13]. However, in these systems, only the lighting directions are changed while the viewing direction is fixed.

In order to perfectly measure BRDFs, both a light source and a sensor must be located at every direction around the target object. A gonireflectometer[6] is a device that can separately rotate a light source and a sensor. However, dense measurement of BRDFs requires excessive amounts

of time because reflected light must be recorded for all combinations of lighting and viewing directions.

In order to dramatically shorten the measuring time, some systems using a mirror have been proposed. Ward[12] proposed a BRDF measuring system which uses a large hemispherical half-mirror and a fish-eye lens. Although omnidirectional reflected lights are observed at once without camera rotation, this system requires a rotational mechanism of the light source behind the hemisphere. Dana[1] constructed a system using a paraboloidal mirror. Although the system can operate with the exclusion of a light source rotational mechanism, a light source translational mechanism remains necessary. Moreover, the range of lighting and viewing directions is limited.

Davis and Rawling as Boeing[2] have patented a device using an ellipsoidal mirror to correct the reflected light using a CCD sensor. Mattison et al. [8] have developed a hand-held instrument to measure BRDF based on the patent. While the patent focuses on only gathering reflected light, the rapid control of the incident direction is not mentioned. Since the incident direction is mechanically varied, the dense and rapid control of the incident direction is difficult.

Recently, Han et al.[4] constructed a system which uses some planar mirrors similar to those used in a kaleidoscope. By combining these mirrors and a projector, BTF (Bidirectional Texture Function) can be measured without any mechanical drive. However, the lighting and viewing directions are few with this system, and therefore dense measurement of BRDF is difficult.

We, on the other hand, propose in this study a new BRDF measuring system which combines an ellipsoidal mirror and a projector. Since our system completely excludes mechanical rotation and translation, high-speed measurement is realized. The system can measure dense BRDFs because both lighting direction and viewing direction are densely changed.

3. BRDF

3.1. Definition of BRDF

To represent reflection properties, the bidirectional reflectance distribution function (BRDF) is used. The BRDF represents the ratio of outgoing radiance in the viewing direction (θ_r, ϕ_r) to incident irradiance from a lighting direction (θ_i, ϕ_i) , as shown in Fig.1. While the BRDF does in fact depend on wavelength, it is sufficient to define the BRDF for each R, G, and B color channel for many applications such as computer graphics. Hence we define the BRDF as a 4-parameter function.

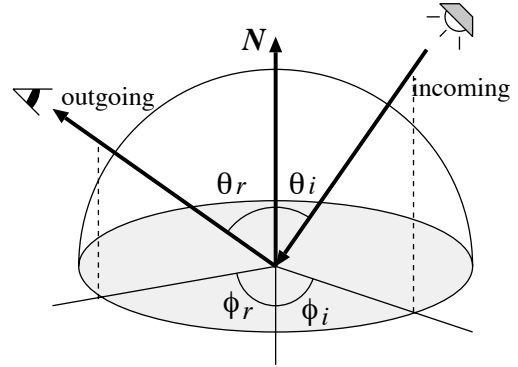


Figure 1. Four angular parameters of BRDF.

3.2. Parametric and non-parametric model

BRDF models can be classified into parametric models and non-parametric models. Parametric models represent reflection properties by mathematical formulations, such as the above-mentioned Phong model[9] and Torrance-Sparrow model[11]. These models formulate reflection properties using a small number of parameters and are suitable for hardware rendering. However, the estimation of parameters in these reflection models is often unstable. Therefore, perfect reproduction of the complex reflection properties of real objects is difficult.

Non-parametric models, on the other hand, directly record real intensities for each direction as values of the reflection function. Since this method can deal with complex reflection properties without error, the BRDFs of a variety of materials can be accurately recorded. Although description requires huge amount of memory, non-parametric models are becoming mainstream as the storage capacities of PCs and demand for generating high quality computer graphics increase.

In our method, we describe the BRDF using a non-parametric model to ensure accuracy.

3.3. Isotropic and anisotropic reflection

When a camera and a light source are fixed, the rotation of an object around the surface normal does not change the appearance of the center point of the rotation for some materials. Such reflection is called isotropic reflection. If we can assume isotropic reflection, then the BRDF can be described using only three parameters, θ_i , θ_r , and ϕ ($\phi = \phi_i + \phi_r$).

On the other hand, there are many materials that change in appearance according to the rotation around the surface normal. Such reflection is called anisotropic reflection, and typical materials of this type are brushed metals and cloth fabrics such as velvet and satin. To perfectly describe anisotropic reflection, therefore, the BRDF should be a 4-

parameter function.

If the number of parameters can be reduced from four to three, then the measuring time and data size can be significantly reduced. However, as the characteristics of clothes cannot be accurately reproduced by the 3-parameter function, we use the 4-parameter function for representing the BRDF in order to realize perfect descriptions of the reflection properties of complex materials such as velvet and satin.

3.4. Problems with 4-parameter description

As described above, in this study we define the BRDF as a 4-parameter function in which the reflection intensities are directly recorded without mathematical formulation, allowing for the dramatic improvement of the ability to express reflection properties. However, there are two major problems associated with 4-parameter description: data size and measuring time.

First, let us consider the problem of data size. If the angles θ_r , ϕ_r , θ_i , and ϕ_i are rotated at one degree intervals, and the reflected light is recorded as R, G, and B color information for each angle, then the required data size is estimated as follows:

$$360 \times 90 \times 360 \times 90 \times 3 = 3,149,280,000 \text{bytes}. \quad (1)$$

It has been generally thought that a data size of 3GB is too large to record. However, a size of 3GB is not impractical as the storage capacities of recent PCs has been increasing significantly. Moreover, BRDFs can be effectively compressed because they include much redundancy. Therefore, data size is not a serious problem.

On the other hand, the problem of measurement time remains serious. The light source must be rotated for every θ_r and ϕ_r , and the sensor must also be rotated for every θ_i and ϕ_i . Since the combinations of lighting angle and sensor angle become extremely great in number, a long measuring time is required. If we assume that the sampling interval is one degree for each lighting angle and sensor angle, then the total number of measurements can be estimated as follows:

$$360 \times 90 \times 360 \times 90 = 1,049,760,000. \quad (2)$$

This means that it would require 33 years to measure all combinations if it takes one second to measure one reflection color. Of course the measuring time can be shortened by using a high-speed camera, but the total time required would still remain impractical. Even if the performance of PCs continues to improve, there is no prospect for solving this problem of measuring time in the near future.

While the problem of data size is not serious, the problem of measuring time warrants consideration. We believe that the reason why there is little research with the aim to measure dense 4-parameter BRDFs is due to this problem of

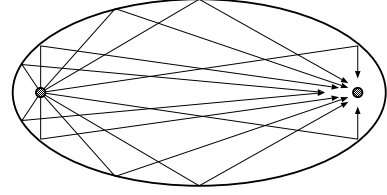


Figure 2. Ellipsoid properties.

measuring time. In this paper, we straightforwardly tackle the problem of measuring time by devising a catadioptric system.

4. BRDF measurement using an ellipsoidal mirror

4.1. Principle of the measuring method

Dense measurement of BRDFs requires huge amounts of time because the measurement is based on the mechanical rotation of the camera and light source around the target object. To realize high-speed measurement, we attempt to exclude the rotation mechanism from the measuring system. To this end, we utilize an ellipsoidal mirror instead of the rotation mechanism.

The ellipsoidal mirror used in our system has a circular cross-section along the Z-axis as defined in Eq.(3). Here, a and b are parameters which decide the size and shape of the ellipsoid. The inner surface of the ellipsoid has specularity.

$$\frac{x^2}{a^2} + \frac{y^2}{a^2} + \frac{z^2}{b^2} = 1 \quad (3)$$

An ellipsoid has two focal points. All rays which pass one focal point reflect onto the ellipsoidal mirror and pass the other focal point, as shown in Fig.2. We utilize this property of ellipsoidal mirrors for measuring BRDFs. A small facet of the target object is placed at a focal point, and a camera is placed at the other focal point. Since the rays reflected from the target object in every direction converge at a single point, all of the rays can be captured using a camera. This means that all reflected rays can be recorded as an image without using a rotation mechanism.

In addition, our system shortens the required changes of lighting direction by combining an ellipsoidal mirror and a projector. The projector serves as a substitute for a light source. Moreover, by placing the projector at the focal point, omni-directional illumination can be realized. However, since both a camera and projector cannot be located at same position, a beam splitter is used. A ray from the projector corresponds to incident light from a certain direction. That is, the lighting direction to the target object can be arbitrarily controlled by changing the projection pattern without the use of any mechanical device. Moreover, since the

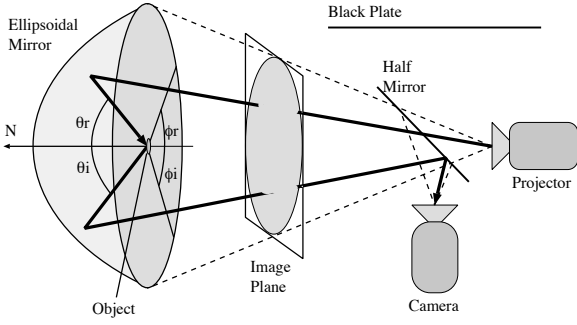


Figure 3. Design of measurement system.

changing of the projecting pattern can be performed more quickly than mechanical rotation, high-speed measurement of BRDFs can be realized.

4.2. Design of the measurement system

Figure 3 shows the design of the measurement system. The component parts are a projector, a camera, an ellipsoidal mirror, and a half-mirror. When the projector illuminates one point, the ray reflects on the ellipsoidal mirror and illuminates the target object from the lighting direction of (θ_i, ϕ_i) . Then, the incident light is reflected on the target object, and the reflected lights to omni-direction are reflected on the ellipsoidal mirror again. Finally, all rays are captured as an image by the camera. The reflected intensity to the viewing direction (θ_r, ϕ_r) is recorded as a single pixel in the captured image.

4.3. Conversion between angle and image location

The lighting direction and the viewing direction are specified as angles. However, the angles are expressed as 2-D locations in the projecting pattern or the captured image. The conversion between the angle and the image location is easy if geometric calibration is done for the camera and the projector. Figure 4 illustrates the relationship between the angle (θ, ϕ) and the image location.

One light source ideally corresponds to one pixel in the projection pattern. However, one pixel does not have enough luminous energy, and therefore the captured image tends to be noisy. Hence, we set a certain size for the light source. If a filled circle is drawn in the projection pattern, then the solid angle from the target object changes according to its location in the projection pattern. To keep the solid angle of the light source constant for every direction, pixels whose directions are within the solid angle are set to white in the projecting pattern, as shown in Fig.5. Although the shape of the light source in the projection pattern is not circular, the solid angle of the light source becomes inde-

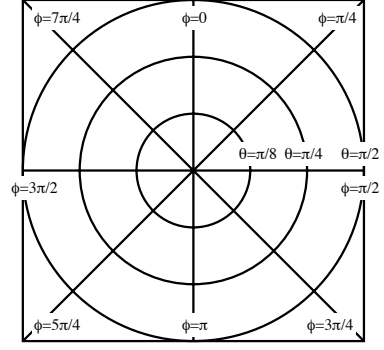


Figure 4. Relationship of the angle and image location.

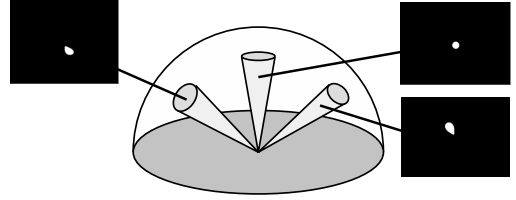


Figure 5. Examples of projection pattern.

pendent to the incident direction.

5. Experimental results

5.1. Simulation using the Ward reflection model

First, we estimated the suitable sampling interval of the four angle parameters $\theta_i, \phi_i, \theta_r,$ and ϕ_r . If we set a small sampling interval, then dense reflection data are obtained. However, the data size and the measuring time increase in inverse proportion to the sampling interval. Therefore, the minimum requirement for sampling interval should be estimated. The sampling interval of the lighting direction corresponds to the number of captured images, and the sampling interval of the viewing direction corresponds to the image size.

For precise estimation, the relationship between the sampling interval and the accuracy is examined by ray tracing simulation. For the simulation, the Ward model as shown in Eq.(4) is used as the anisotropic reflection model.

$$\rho(\theta_i, \phi_i; \theta_r, \phi_r) = \frac{\rho_d}{\pi} + \frac{\rho_s}{4\pi\alpha_x\alpha_y\sqrt{\cos\theta_i\cos\theta_r}} e^{-\tan^2\theta_h \left(\frac{\cos^2\phi_h}{\alpha_x^2} + \frac{\sin^2\phi_h}{\alpha_y^2} \right)} \quad (4)$$

Here, ρ_d and ρ_s denote the diffuse reflectance and the specular reflectance, respectively. α_x and α_y denote the standard deviation of the surface slope in the x and y direction, respectively. We set α_x to be 0.05 and α_y to be 0.16 to express anisotropic reflection. These values are shown in [12]

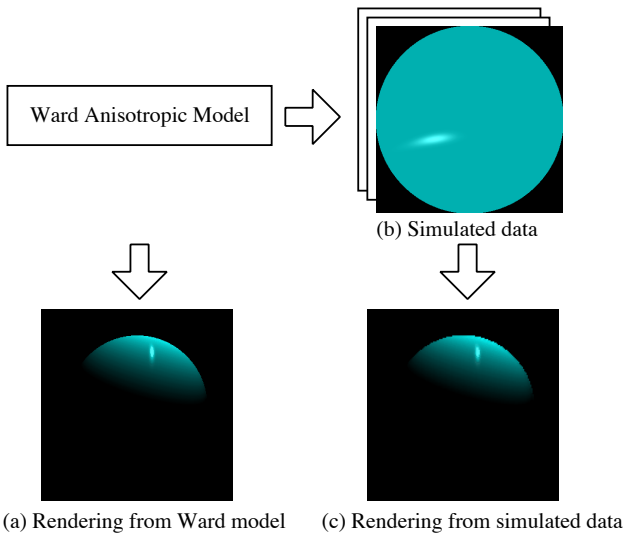


Figure 6. Simulation by ray tracing.

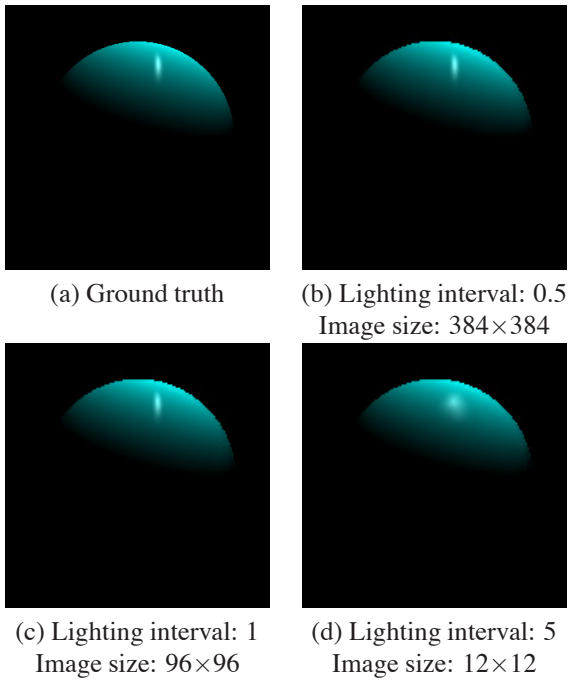


Figure 7. CG images under various sampling conditions.

as a reflectance of rolled brass.

Figure 6 illustrates how to compare the quality of the simulated images. (a) is the ground truth of a rendered sphere directly generated using the reflection model of Eq.(4). (b) shows a set of simulated images expected to be captured by the proposed measuring system. (c) shows a rendered sphere generated from the simulation data of (c). By comparing (a) and (c), the effect of the sampling interval is evaluated. In this experiment, the size of the gener-

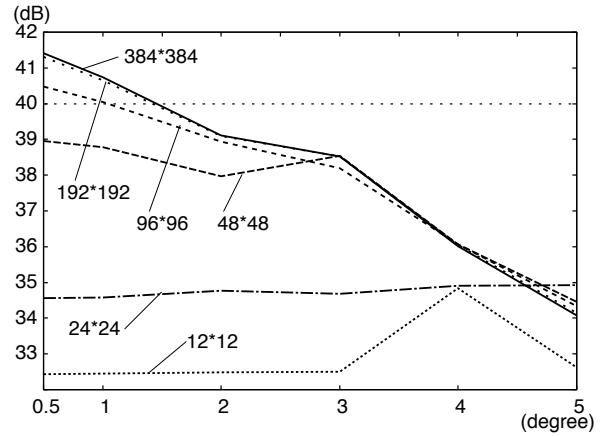


Figure 8. Relationship between lighting interval and PSNR.

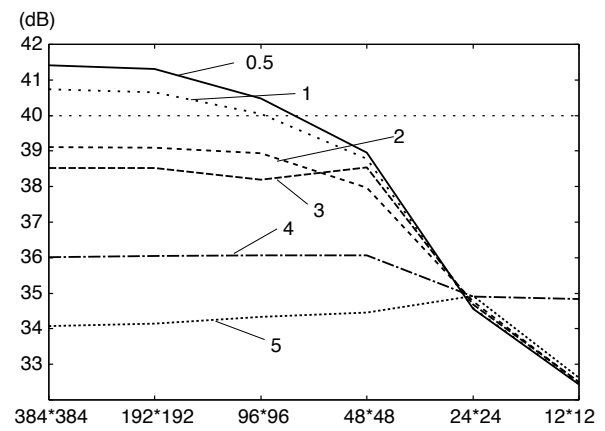


Figure 9. Relationship between image size and PSNR.

ated image of (a) and (c) is 160×160 , and the camera is fixed. The lighting direction of the sphere image is set to 19×10 directions: 19 directions for rotation from the viewing direction to the overhead direction, and 10 directions for rotation around the viewing direction. Figure 7 shows some examples generated with changing sampling intervals. We can see that a large sampling interval causes poor reproducibility of specular reflections.

To quantitatively evaluate the differences of images, PSNR (Peak Signal to Noise Ratio) is calculated for each Y, Cb, and Cr component. Figure 8 shows the minimum PSNR when the sampling interval of the lighting direction varies. Each line in the graph indicates the size of the captured image. Figure 9 shows the minimum PSNR when the size of the captured image varies. Each line in the graph indicates the sampling interval of the lighting direction.

The Cb and Cr components maintain a large PSNR, while the Y component always has the lowest PSNR. The reasons for this are that the color does not change even if the sampling interval is large and that the Y component tends

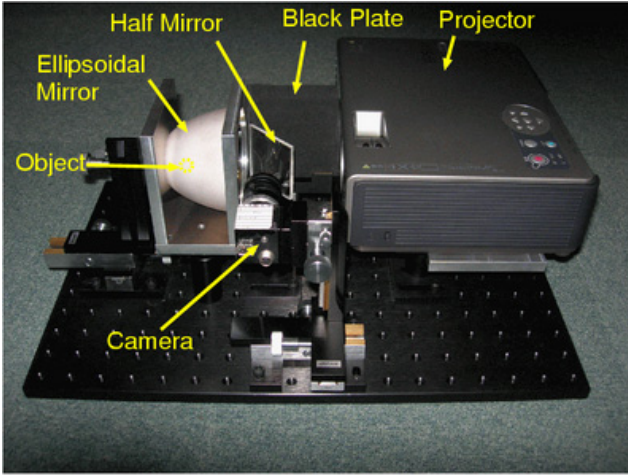


Figure 10. BRDF measuring system: RCG-1.



Figure 11. Ellipsoidal mirror.

to be affected by slight differences in specular reflection. In fact, specular reflections are not accurately reproduced when the sampling interval of the lighting direction is large.

It is generally believed that we cannot perceive noise if the PSNR is more than 40dB. This minimum PSNR becomes greater than 40dB when the sampling interval of the lighting direction becomes smaller than 1 degree and the image size becomes larger than 96×96 . The sampling interval of 1 degree corresponds to the 32400 images, while the image size of 96×96 corresponds to the density of the viewing direction, although the angle is not uniform because the density of θ_r varies according to ϕ_r , as shown in Fig.4. Based on this simulation, we found that under typical conditions of BRDF measurement, the sampling interval of the lighting direction should be less than 1 degree and the image size should be larger than 96×96 . We regard these conditions as a rough standard and use the same condition in the following section.

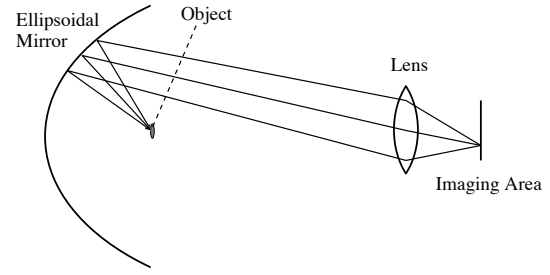


Figure 12. Light path with focusing.

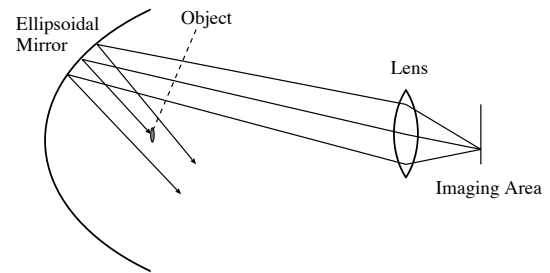


Figure 13. Light path without focusing.

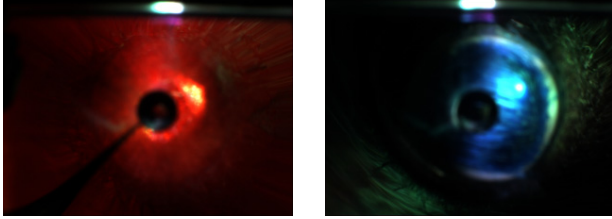
5.2. Prototype system

Figure 10 shows the proposed BRDF measuring system, named RCG-1 (Rapid Catadioptric Gonioreflectometer). This system includes an IEEE-1394 camera (Point-Grey Flea), a liquid crystal projector (EPSON EMP-760), and an ellipsoidal mirror (Melles Griot). These components are manually aligned based on the manufacturing specifications. In this system, we assume that the projecting intensity is spatially uniform. Since we set no gamma correction for capturing image by the camera, the linearity of the intensity is guaranteed.

Since this ellipsoidal mirror has a hole at the edge of the long axis as shown in Fig.11, the BRDFs within $0 \leq \theta_i, \theta_r \leq 27$ can not be measured¹. A small facet of the target object is placed at the focal point by using a piano wire. Since the piano wire is very thin and the location of the wire is known, the missing data caused by the wire can be easily interpolated from neighboring data.



(a) velvet (b) satin
Figure 14. Target objects (velvet and satin).



(a) velvet (b) satin
Figure 15. Examples of captured image.

5.3. Focusing

We will now consider the focusing of the projector and the camera. The projection ray intuitively seems to be focused on the target object, as shown in Fig.12. In this case, one pixel in the projecting pattern is observed as a light source having a large solid angle. The solid angle is decided by the size of the lens. To avoid this undesired effect, the rays from the projector are focused at infinity, as shown in Fig.13 in our system. Through the defocus of the projection, the light source is observed as a point from the position of the target object. In order to observe only a small area on the target object by the camera, we used a camera with a narrow aperture.

5.4. BRDFs of satin and velvet

In this section, we show the results of measured BRDFs using the proposed RCG-1 system. The target objects are velvet and satin, both of which have anisotropic reflections, as shown in Fig.14.

First, we evaluated the measuring time. The sampling interval was set to 1 degree based on the preliminary experiments in Sec.5.1. Pattern corresponding to the lighting directions $\theta_i = 30$ and $\phi_i = 250$ were projected, and the reflected images were captured, as shown in Fig.15 (a) and (b) for velvet and satin, respectively. It is noted that some BRDFs could not be measured because of the hole of the el-

¹If the BRDFs are measured while changing the surface normal direction of the target object, the missing data can be complemented by merging the BRDFs. Now we are constructing a new BRDF measuring system so that perfect BRDFs are measured.

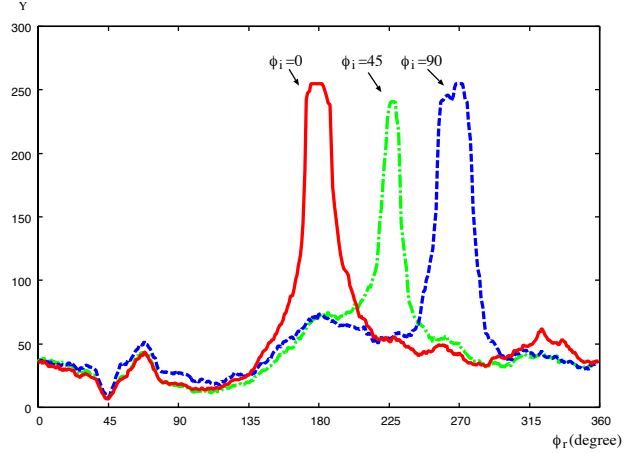


Figure 16. Reflectance of velvet.

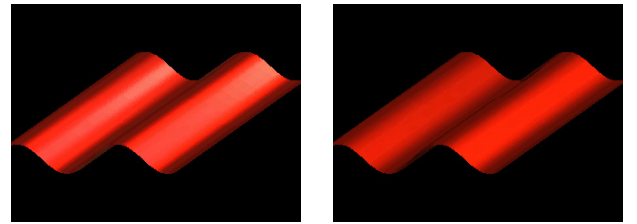


Figure 17. Rendering results of velvet.

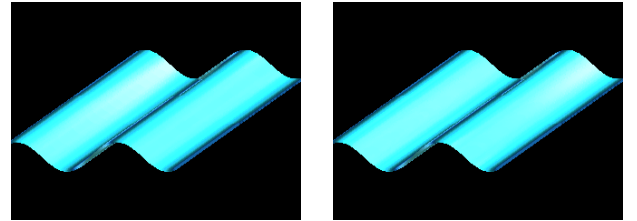


Figure 18. Rendering results of satin.

lipsoidal mirror. We captured $360 \times 90 = 32400$ images for each material. The time required was 0.18 sec/image, for a total measuring time of about 50 minutes. A major part of the measuring time was occupied by the process of preparing the projection pattern and recording the captured image.

Next we show the results of measured BRDFs using the RCG-1 system. Figure 16 shows the change of reflection intensities of the velvet material when θ_r is fixed to 30 degrees and ϕ_r rotates from 0 to 360 degrees. In the graph, the three lines show the respective reflection intensities for the lighting direction (θ_i, ϕ_i) : $(30, 0)$, $(30, 45)$, and $(30, 90)$. We can see that the three lines have different shapes at their peaks which represent the characteristics of the specular reflection. Since the velvet material has anisotropic reflection properties, the reflectance varies even if the relative angle

$(\phi_r - \phi_i)$ is the same.

Finally, we show some computer graphics results using our system to demonstrate a possible application of our proposed system of measuring BRDFs. Images of a corrugated plane are rendered using the measured BRDFs. Figures 17 and 18 are generated images of velvet and satin under different illumination conditions. The rendering process of this corrugated shape does not require the missing data fortunately. We can see that the characteristics of anisotropic reflection are reproduced. To improve the quality of the measured BRDFs, more accurate calibration is necessary.

5.5. Discussion

Since the proposed system is the first prototype for measuring BRDFs, we evaluated only the measuring time in this paper. There are several unresolved issues.

First, we have to evaluate the measured BRDFs numerically to check the accuracy of the measuring device. For the evaluation, we are trying to compare the measured BRDFs and the ground truth by using reflectance standards whose reflection properties are known. By the comparison, we can evaluate the accuracy of the geometric and photometric calibration of the camera and the projector. Another idea for the evaluation is to check whether the data satisfy the principle of Helmholtz reciprocity.

To widen dynamic range of BRDFs is also very important. The limited dynamic range is a problem because we cannot measure strong specular highlights and weak diffuse reflections simultaneously. We are trying to solve this problem by using a high dynamic range camera.

6. Conclusion

In this paper, we proposed a new high-speed BRDF measurement system that combines an ellipsoidal mirror with a projector. The proposed system can measure complex reflection properties including anisotropic reflection. Moreover, the measuring time of BRDFs can be significantly shortened by the exclusion of a mechanical device. The combination of an ellipsoidal mirror and a projector enables fast changes in lighting direction.

Although the proposed system can enable high-speed BRDF measurement, the measuring time remains at approximately fifty minutes. Thus, one of the tasks of our future work will be to further shorten the measuring time. The adaptive change of the sampling intervals may be effective to speed up.

In this paper, we focused only on the BRDF measuring speed by the developed system. We have to evaluate measured BRDFs numerically, and solve the narrow dynamic range problem. We are currently working on these issues with the aim of realizing a measuring system suitable for many practical applications.

References

- [1] K. J. Dana, "BRDF/BTF Measurement Device", Proc. International Conference on Computer Vision (ICCV2001), Vol.2, pp.460-466, 2001.
- [2] K. J. Davis and D. C. Rawlings, "Directional reflectometer for measuring optical bidirectional reflectance", United States Patent 5637873, June, 1997.
- [3] P. Debevec, T. Hawkins, C. Tchou, H. P. Duiker, W. Sarokin, and M. Sagar, "Acquiring the Reflectance Field of a Human Face", Proc. SIGGRAPH2000, pp.145-156, 2000.
- [4] J. Y. Han and K. Perlin, "Measuring Bidirectional Texture Reflectance with a Kaleidoscope", ACM Transactions on Graphics, Vol.22, No.3, pp.741-748, 2003.
- [5] T. Hawkins, J. Cohen, and P. Debevec, "A Photometric Approach to Digitizing Cultural Artifacts", Proc. International Symposium on Virtual Reality, Archaeology, and Cultural Heritage, pp.333-342, 2001.
- [6] H. Li, S. C. Foo, K. E. Torrance, and S. H. Westin, "Automated three-axis gonioreflectometer for computer graphics applications", Proc. SPIE, Vol.5878, pp.221-231, 2005.
- [7] T. Machida, N. Yokoya, and H. Takemura, "Surface Reflectance Modeling of Real Objects with Interreflections", Proc. International Conference on Computer Vision (ICCV2003), Vol.1, pp.170-177, 2003.
- [8] P. R. Mattison, M. S. Dombrowski, J. M. Lorenz, K. J. Davis, H. C. Mann, P. Johnson, and B. Foos "Handheld directional reflectometer: an angular imaging device to measure BRDF and HDR in real time", Proc. SPIE Vol. 3426, p. 240-251, 1998.
- [9] B. T. Phong, "Illumination for Computer Generated Pictures", Commun. ACM, vol.18, pp.311-317, 1975.
- [10] Y. Sato, M. Wheeler, and K. Ikeuchi, "Object Shape and Reflectance Modeling from Observation", Proc. SIGGRAPH'97, pp.379-387, 1997.
- [11] K. E. Torrance and E. M. Sparrow, "Theory for off-specular reflection from roughened surface", J. Opt. Soc. Am, vol.57, pp.1105-1114, 1967.
- [12] G. J. Ward, "Measuring and Modeling anisotropic reflection", Proc. SIGGRAPH'92, pp.255-272, 1992.
- [13] A. Wenger, A. Gardner, C. Tchou, J. Unger, T. Hawkins, and P. Debevec, "Performance Relighting and Reflectance Transformation with Time-Multiplexed Illumination", Proc. SIGGRAPH2005, pp.756-764, 2005.